Oil Shale, 2026, 43, 2, 228–240 https://doi.org/10.3176/oil.2026.2.05

Methylation of kukersite kerogen – estimation of the content of free hydroxyl groups

Kristi Rõuk[(a)]*, Mariliis Kimm[(a)], Kristiina Kaldas[(a)], Ivo Heinmaa[(b)], Tõnis Pehk[(b)], Estelle Silm[(a)], Margus Lopp[(a)]

[(a)] Industrial Chemistry Laboratory, Department of Chemistry and Biotechnology, School of Science, Tallinn University of Technology, Ehitajate tee 5, 19086 Tallinn, Estonia

[(b)] National Institute of Chemical Physics and Biophysics, Akadeemia tee 23, 12618 Tallinn, Estonia

Received 25 October 2025, accepted … 2026, available online … 2026

Abstract. *Derivatization of the kerogen backbone changes its chemical reactivity profile. In this study, kukersite kerogen was methylated with dimethyl carbonate. The substance was analyzed before and after processing by Fourier transform infrared spectroscopy, ^{13}C cross-polarization/magic angle spinning nuclear magnetic resonance spectroscopy, and elemental analysis. It was observed that kukersite kerogen can be readily methylated with dimethyl carbonate. Based on mass balance and the Lille-Blokker model, an average of 19 methyl groups were added to the kerogen unit. It was concluded that about half of the hydroxyl groups in Estonian kukersite kerogen are "free" and accessible to methylation.*

Keywords: *kukersite, kerogen, methylation, hydroxyl group, dimethyl carbonate, FTIR, NMR.*

1. Introduction

Kukersite is a sedimentary rock found in northern Estonia that contains about 30–50% of organic matter called kerogen [1, 2]. Throughout the 20th century, kukersite was mainly used for energy production through combustion and for oil extraction via thermal cracking [3]. However, it is now widely accepted that the traditional uses of oil shale have exhausted their potential and fail to meet contemporary environmental and efficiency standards. Instead, kukersite could be used as a versatile source of organic matter and various chemical structures.

* Corresponding author, kristi.rouk@taltech.ee

It is generally accepted that Estonian kukersite, formed during the Ordovician period over 450 million years ago, originates from colonies of *Gloeocapsomorpha prisca* which were rich in resorcinolic units [4]. Building on this, Lille proposed in 1999 that the resorcinolic units form the structural backbone of kukersite kerogen [5]. Two structural models of kerogen have since been independently proposed by Blokker et al. [6] and Lille et al. [1, 7]. More recently, a new model based on the Lille model was developed by Chu et al. (here Lille–Chu model) [8] and a generalized Lille–Blokker model, which integrates elements of both original frameworks, was proposed by our group [9]. However, the number of free hydroxyl groups per kerogen unit is not exactly defined in any of these models. The content of free hydroxyl groups is 24% in the Blokker model [6], 43% in the Lille model [1, 7], 47% in the Lille–Chu model [8], and 50% in the generalized Lille–Blokker model [9]. Yet, the hydroxyl group is a crucial functionality that strongly influences the chemical properties and reactivity of kukersite kerogen. Thus, the information regarding the amount of free hydroxyl groups in kukersite is essential.

Such knowledge may be obtained through the chemical alteration of kerogen, examined in a recent review [10]. However, few papers investigate the chemical reactions of kukersite kerogen systematically. In contrast, this topic has been extensively studied in lignin, a wood-derived biopolymer [11–13], and other natural materials [14–16]. Given the structural similarities between lignin and kerogen, such as shared functional groups and low solubility [17, 18], lignin studies may offer valuable insights for kerogen derivatization.

Alkylation, particularly methylation, is one of the most common chemical reactions for protecting hydroxyl groups. This has been extensively studied

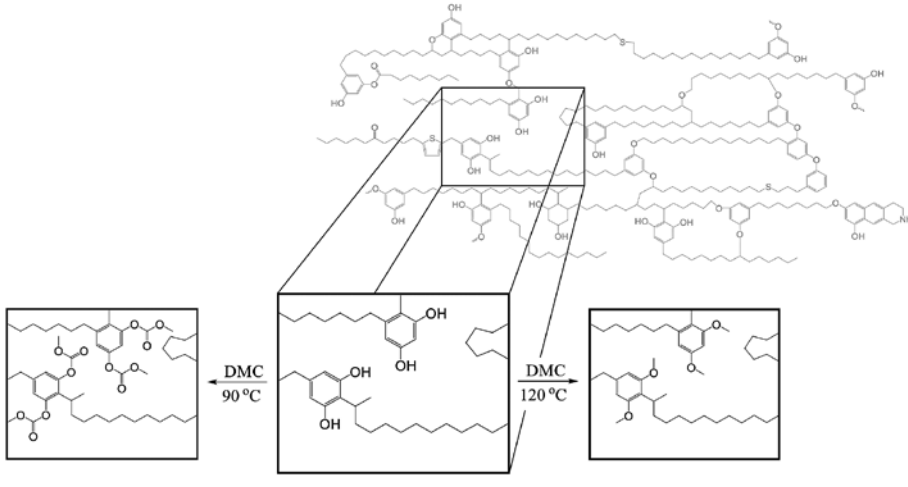

Fig. 1. Treating kerogen with dimethyl carbonate (DMC) could result in methoxycarbonylation at 90 °C and methylation at 120 °C or higher [25].

in lignin, employing methylating agents such as alkyl halides [19], dimethyl sulfate [20], trimethyl phosphate [21], and dimethyl carbonate [22, 23]. However, only one attempt to alkylate kukersite kerogen has been reported [24].

In this paper, we present our work on the methylation of kerogen using an eco-friendly methylating agent, dimethyl carbonate (DMC). DMC has dual reactivity: at 90 °C, it methoxycarbonylates hydroxyl groups, whereas at 120 °C and above, methylation occurs [25]. Kukersite was subjected to both reaction conditions (see Fig. 1). The resulting derivatized kerogen was analyzed by using Fourier transform infrared spectroscopy (FTIR), ^{13}C cross-polarization/magic angle spinning nuclear magnetic resonance spectroscopy (^{13}C CP MAS NMR), and elemental analysis. The number of free hydroxyl groups in a kerogen fragment was quantitatively estimated based on the Lille–Blokker model.

2. Materials and methods

2.1. Materials

All experiments were carried out on kukersite kerogen concentrate powder (91.3% kerogen content, particle size ≥ 45 μm), obtained from the Oil Shale Competence Center in Kohtla-Järve, Estonia. The material was dried at 105 °C to constant mass before use. Additional details regarding the preparation method of the kerogen concentrate are available in an article previously published by our research group [26]. All other chemicals were used as purchased without any further treatment or purification.

2.2. Experimental procedures

2.2.1. Methylation of kerogen: general procedure

The methylation method of Sen et al. [22] was applied with slight modifications.

The reactions were carried out in a 100 mL pressure reactor (stainless steel 4566C, Parr Instrument Company, Moline, Il, USA).

To the reactor with 1.0 g of kerogen and solid 0.5 g of NaOH (12.5 mmol), 25 mL of DMC (297.8 mmol) was added. The reactor was heated to 200 °C under a nitrogen atmosphere while stirring at 250 rpm. The reaction time was measured from the moment the temperature reached 190 °C. After a defined reaction time (5 h and 24 h), the reactor was cooled to room temperature, depressurized, and the liquid phase was separated by centrifugation. To the remaining solid phase, 50 mL of a 1:2 acetone–water mixture was added, and the mixture was centrifuged. This washing step was repeated three times until the pH reached 6–7, and the solid was dried to constant mass.

2.2.2. Methylation of kerogen: quantitative procedure

To the reactor with 1.000 g of kerogen and 0.5 g of NaOH (12.5 mmol), 25 mL of DMC (297.8 mmol) was added. The reaction mixture was heated to 200 °C under a nitrogen atmosphere while stirring at 250 rpm for 24 h. Then the reactor was cooled to room temperature, depressurized, and the phases were separated by centrifugation. The liquid phase was orange-brown in color. It was suggested that the kerogen slightly degraded at 200 °C and the resulting organic matter leached to the liquid phase.

The solid phase was washed with 4 × 15 mL DMC and separated by centrifugation. The combined liquid phases were concentrated to yield 33.2 mg of dark brown oil. The solid phase was further washed with 4 x 50 mL of distilled water, until the pH reached 6–7, and separated by centrifugation. To minimize the loss of methylated product, the liquid phase was additionally filtered when necessary. The obtained solid mass and the oily mass from DMC extraction were combined and dried to constant mass on a rotary evaporator, yielding 1.043 g of methylated kerogen.

2.2.3. Methoxycarbonylation of kerogen

To the pressure reactor with 1.0 g of kerogen and 0.5 g of NaOH (12.5 mmol), 25 mL of DMC (297.8 mmol) was added. The reaction mixture was heated to 90 °C under a nitrogen atmosphere while stirring at 250 rpm for 24 h. Then the reactor was cooled to room temperature and depressurized. The reaction mixture was filtered, and the obtained solid was sequentially washed with distilled water, ethanol, and diethyl ether. Finally, it was dried under vacuum to constant mass.

2.3. Analytical methods

The FTIR spectra were recorded on an IRTracer-100 FTIR spectrophotometer (Shimadzu, Japan). Transmission spectra (KBr pellets with kerogen 100:1) were measured in the range 400–4000 cm^{-1} with a resolution of 2 cm^{-1} by accumulating 30 scans. The same parameters were used in attenuated total reflectance mode.

^{13}C CP MAS NMR spectra were recorded on a Bruker AVANCE-II spectrometer at a 14.1 T magnetic field using a home-built double resonance magic-angle-spinning probe for 4 × 25 mm Si_3N_4 rotors. The spinning speed of the sample was set to 12.5 kHz with an ordinary cross-polarization (CP) pulse sequence, where the duration of the ramped polarization transfer pulse was 2 ms, and the relaxation delay between the excitations was 5 s. The intensities in the spectra were normalized to the weight of the sample and to the number of accumulations.

The CHNS elemental analysis was conducted with an Elementar vario MICRO cube.

3. Results and discussion

3.1. FTIR spectra

FTIR spectra of the kukersite kerogen concentrate powder were recorded using both transmission and attenuated total reflectance (ATR) modes. The obtained spectra were similar and closely resembled those reported by Derenne et al. [27, 28] and Blokker et al. [6]. Although the ATR technique yields weaker signals, it was selected for subsequent measurements due to its simplicity and lower sensitivity to moisture, which enables more accurate monitoring of changes in hydroxyl peak intensity.

Methylated kerogen was prepared according to the general procedure. FTIR spectra were recorded for samples of initial kerogen (a), and methylated kerogen from 5 h (b) and 24 h (c) reactions (Fig. 2). Considerable differences were observed in the spectra of the methylated samples compared to the initial kerogen. Most importantly, in spectrum (b), the characteristic absorption band at 3400 cm^{-1}, corresponding to hydroxyl groups, had significantly diminished. Additionally, a decrease in the bands at 1350 cm^{-1} and 1020 cm^{-1} was observed, further confirming the loss of hydroxyl groups. A new band at 1265 cm^{-1}, attributed to the newly formed phenyl methyl ether bonds, was also noted. In addition, a symmetric C–H stretching band characteristic of methoxy

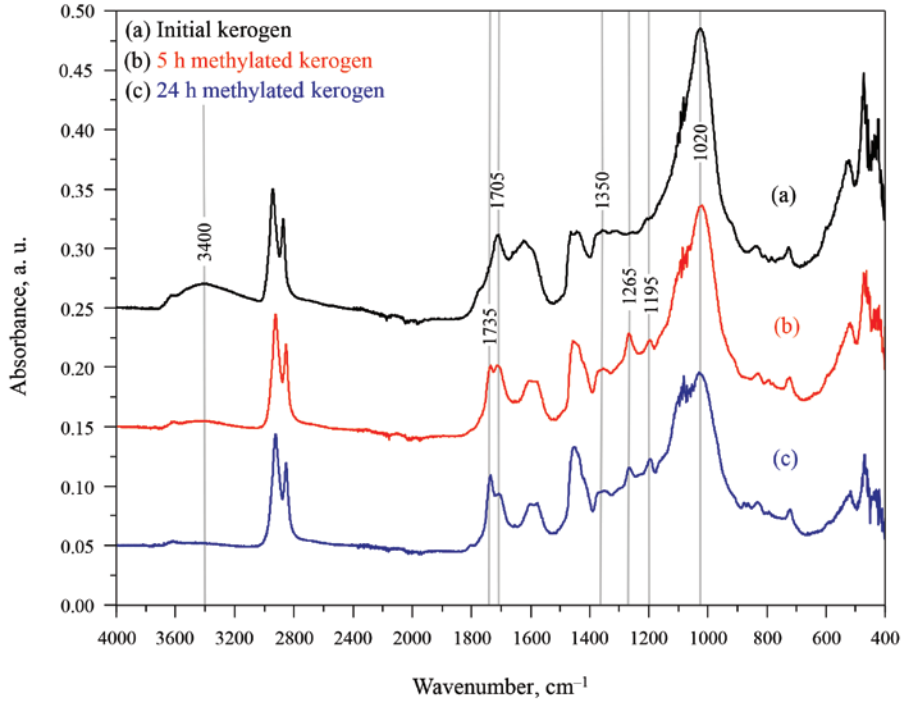

Fig. 2. ATR-FTIR spectra of Estonian kukersite kerogen concentrate measured before, after 5 h, and after 24 h of methylation.

groups at 2840–2820 cm^{-1} and an aliphatic C–O stretching band at 1050–1010 cm^{-1} were expected [29]. However, those bands were likely masked by the relatively more intense bands of the kerogen structure. Similarly, the band at 1705 cm^{-1}, corresponding to carboxyl and carbonyl groups, had slightly decreased in both spectra, and new bands appeared in the 1735 cm^{-1} and 1195 cm^{-1} regions, which may correspond to the formation of aliphatic esters. These changes were even more pronounced in spectrum (c).

Titration data reported by Aarna and Lippmaa [24] suggest that one kerogen "molecule" contains ~0.8 carboxyl groups. Therefore, the ester bands may correspond to the esterified native carboxyl groups. However, the methoxycarbonylation of kerogen could also account for these absorption bands. This theory was tested in a separate experiment, further discussed in the next paragraph. Another possible explanation for the appearance of these bands is degradation of the kerogen structure, which may lead to side reactions and the formation of methyl esters. While rapid kerogen degradation typically occurs at 320–340 °C, it can begin as early as 170–180 °C – well below our reaction temperature of 200 °C [30–32]. Indeed, the liquid phase of the reaction mixture had an orange-brown hue and, upon concentration, produced a small amount of brown, oily substance – likely resulting from degradation – which was not analyzed further. Beyond this observation, no further evidence of degradation was detected, suggesting that although some pyrolysis occurred, its extent was minimal and did not have a significant effect on the results. It may be concluded that ATR-FTIR is a simple and convenient method to track the methylation of kerogen and qualitatively estimate the depth of the process.

3.2. ^{13}C CP MAS NMR spectra

^{13}C CP MAS NMR spectra were recorded for both the initial Estonian kukersite kerogen concentrate and the 5 h and 24 h methylated samples (Fig. 3). It was observed that the spectra of the native Estonian kukersite kerogen resemble those reported by Derenne et al. [27] and Lille et al. [7]. Numerous signals were observed in the region of aliphatic carbon, with a maximum at 30 ppm. The signals at 75 ppm correspond to various non-aromatic carbons adjacent to oxygen atoms, such as oxy-methylene, oxy-methine, and oxy-quaternary carbons. In the region of aromatic carbons, a peak observed at 109 ppm is attributed to the carbons within an aromatic ring adjacent to an oxygen-bearing carbon. The peak at 141 ppm is assigned to aromatic carbons at branching, while the peak at 156 ppm is assigned to carbons within aromatic rings bearing oxygen substituents. The peak at 208 ppm belongs to carbonyl carbons. The asterisks denote the spinning sidebands from the main peaks at 156 and 141 ppm.

The integral number of aliphatic carbons accounts for 74% of the total carbon content, leaving 26% to aromatic carbons, with resorcinols as the main

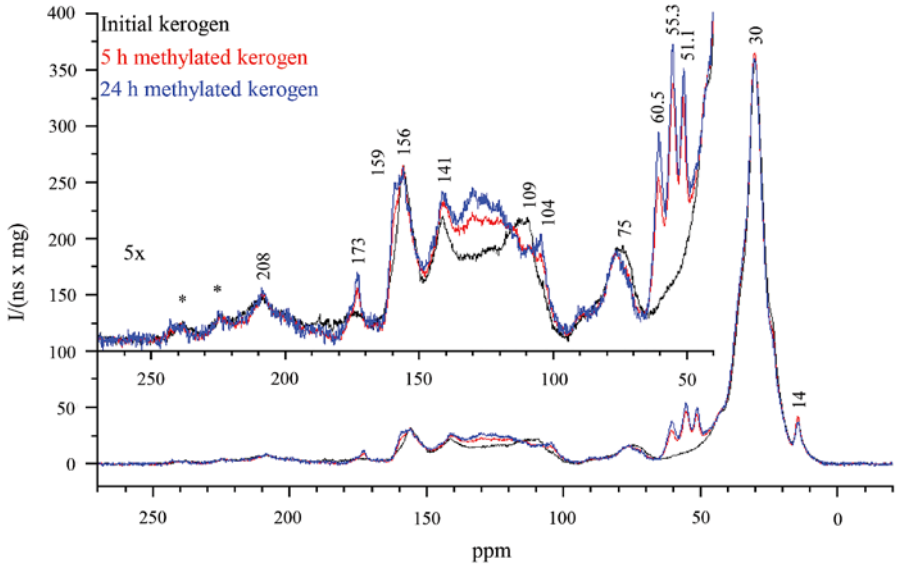

Fig. 3. ^{13}C CP MAS NMR spectra of Estonian kukersite kerogen before and after methylation.

aromatics in kerogen. The latter value is slightly higher than the estimate previously reported by Aarna and Lippmaa (19%) [24] and comparable to that of Lille et al. (24%) [33].

The spectra of 5 h and 24 h methylated kerogen show several changes compared to initial kerogen, which can be traced by calculating and comparing the chemical shifts for simple molecule models (Fig. 4). In the region of aliphatic carbons, three new peaks were observed at 51.1, 55.3, and 60.5 ppm, which should belong to the newly formed methoxy groups. Namely, the peak at 51.1 ppm may be assigned to methylated aliphatic and non-hindered aromatic carboxyl groups, and the peaks at 55.3 and 60.5 ppm to the methylated resorcinolic hydroxyl groups. Specifically, the peak at 55.3 ppm corresponds to sterically unhindered methoxy groups, whereas the peak at 60.5 ppm arises from methoxy groups that are sterically hindered due to ortho-disubstitution on the aromatic ring.

In the region of aromatic carbons, we noticed that the peak at 104 ppm had grown, while the peak at 109 ppm had diminished. In addition, a new shoulder for the peak at 156 ppm, denoting methoxy-substituted aromatic carbons, had appeared at 159 ppm. Both changes can be attributed to the changes in the chemical environment brought on by the added methyl groups. The peak at 173 ppm, initially assigned to carboxyl carbons, had also grown, possibly due to the formation of esters.

The 24 h methylated kerogen spectrum shows the same changes that were observed for 5 h methylated kerogen; however, the peaks are slightly more

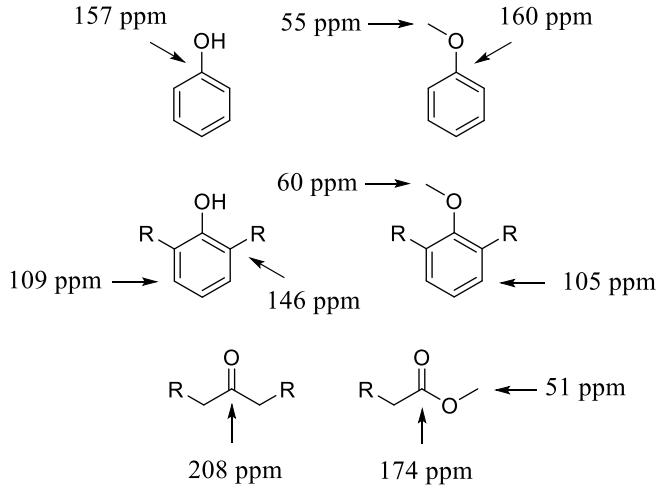

Fig. 4. Calculated chemical shifts of phenols and methylated phenols.

developed. This is a strong indication that the reaction has almost completed within 5 h and matured within 24 h. The NMR spectra also confirm the methylation of kerogen and indicate that both resorcinolic and acidic hydroxyl groups were methylated.

To elucidate the appearance of the methyl ester signals in both IR and NMR spectra, the possibility of kerogen methoxycarbonylation with dimethyl carbonate was investigated. In the product obtained after 24 h of heating at 90 °C, almost no changes were observed in the FTIR spectrum. The expected bands at 1750–1730 cm^{-1} and 1280–1240 cm^{-1} [34, 35] did not appear, and only a slight decrease of the hydroxyl band was observed. Similarly, the characteristic peaks of the methoxycarbonylated product at 157 and 55 ppm were absent from the NMR spectrum. The main changes observed were two sharp peaks at 172.1 and 167.7 ppm, along with a small bump at ~180 ppm, which could not be attributed to methoxycarbonylation.

The obtained results suggest that the methoxycarbonylation reaction proceeds only to a very small extent, if at all.

3.3. Elemental analysis

The elemental composition of the initial Estonian kukersite kerogen concentrate aligned relatively well with our previous measurements [26] as well as previously published results [36]. The elemental compositions of both the native and the methylated kerogens treated for 5 h and 24 h are presented in Table 1.

Table 1. Elemental composition of both native and methylated kerogens after 5 h and 24 h of treatment

	N, %	C, %	H, %	S, %
Native kerogen*	0.30 ± 0.01	66.42 ± 0.21	8.03 ± 0.09	1.41 ± 0.07
5 h methylated kerogen*	0.22 ± 0.01	67.78 ± 0.02	8.08 ± 0.05	1.35 ± 0.10
24 h methylated kerogen*	0.25 ± 0.01	71.03 ± 0.08	8.49 ± 0.01	0.97 ± 0.02

* Mean value of three measurements.

Compared to the elemental composition of the initial kerogen, the carbon and hydrogen contents of the 5 h methylated kerogen were markedly higher. The carbon content had increased by 1.36%, while the hydrogen content had increased by 0.05%. In the 24 h methylated kerogen sample, the carbon and hydrogen contents had increased even more, by 4.61% and 0.46%, respectively. These results are consistent with the changes we expected to occur during methylation.

3.4. Calculation of the number of hydroxyl groups in a kerogen molecule – comparison of the different kerogen structural models

Based on the assumption that the reaction had completed in 24 h, it is possible to calculate the number of hydroxyl groups per "molecule" of kerogen. However, all existing models – the Lille model [7], the Blokker model [6], the Lille–Chu model [8], and the Lille–Blokker model [9] – assign slightly different molecular masses to the kerogen "molecule": 6581 Da, 5312 Da, 5131 Da, and 5650 Da, respectively.

We obtained 1.043 g of methylated product from 1.000 g of starting material. The starting material, with a kerogen content of 91.3%, contained 0.913 g of organic matter and 0.087 g of inorganic matter. Assuming that the latter is inert, the treated sample contains 0.956 g of methylated kerogen. The added methyl groups (actual added mass of CH_2) have a molar mass of 14.027 g/mol. Thus, as shown in equation (1), the amount of added methyl groups is 3.044 mmol. The amount of initial kerogen, calculated using the molecular mass assigned by the Lille–Blokker model, is 0.162 mmol, and the number of methyl groups added to one kerogen "molecule" is 19.

$$n_{\mathrm{CH_3}} = \frac{m_{\mathrm{CH_3}}}{M_{\mathrm{CH_3}}} = \frac{0.956\ \mathrm{g} - 0.913\ \mathrm{g}}{(1 \times 12.011 + 2 \times 1.008)\ \mathrm{g/mol}} \times 1000 = 3.044\ \mathrm{mmol} \quad (1)$$

Similar calculations using the Lille, Blokker, and Lille–Chu models result in 22, 18, and 19 hydroxyl groups per kerogen "molecule," respectively (Table 2).

Table 2. Quantification of free hydroxyl groups: model vs. experimental

	Empirical formula	Free hydroxyl groups counted from the model	Free hydroxyl groups calculated from methylation data for the model
Blokker model	$C_{351}H_{548}O_{34}$	8	18
Lille model	$C_{420}H_{636}O_{44}S_4ClN$	19	22
Lille–Chu model	$C_{366}H_{548}O_{35}S_3ClN$	20	19
Lille–Blokker model	$C_{367}H_{567}NO_{35}S_3$	16	19

These results show that all four models slightly underestimate the number of free hydroxyl groups in kerogen. Moreover, approximately half of the oxygen atoms in the kerogen "molecule" are accessible to methylation. Given that there is only ~1 carboxyl group present per kerogen "molecule," its contribution to methyl group consumption is minimal. The content of "free" hydroxyl groups is quite well represented in the Lille, Lille–Chu, and Lille–Blokker models.

4. Conclusions

In this paper, we have demonstrated that kukersite kerogen can be readily and almost quantitatively methylated using dimethyl carbonate, an environmentally benign methylating agent. No evidence of relevant side reactions, namely methoxycarbonylation, was observed. The study also revealed that all existing structural models of kukersite kerogen might slightly underestimate the amount of free hydroxyl groups in kerogen. Our experiments showed that free hydroxyl groups account for nearly half of the oxygen atoms present in a kerogen "molecule." This selective methylation reaction of kerogen hydroxyl groups paves the way for further studies of other derivatization reactions and potential applications of kukersite derivatives in future valorization efforts.

Data availability statement

The authors confirm that the data supporting the findings of this study are contained within the article. Additional information and original spectra are available on request from the authors.

Acknowledgments

This work was co-funded by the European Union and the Estonian Research Council via project TEM-TA128, supported by the Ministry of Education and Research Centers of Excellence grant TK228 (Center of Excellence in the Circular Economy for Strategic Mineral and Carbon Resources), by Estonian Research Council grant PRG1702, and by Tallinn University of Technology. The authors also thank Angelika Närep and Kati Muldma for conducting elemental analysis measurements, and other colleagues at the Industrial Chemistry Laboratory, Tallinn University of Technology, for their support. The publication costs of this article were partially covered by the Estonian Academy of Sciences.

References

1. Lille, Ü. Current knowledge on the origin and structure of Estonian kukersite kerogen. *Oil Shale*, 2003, **20**(3), 253–263. https://doi.org/10.3176/oil.2003.3.03
2. Veiderma, M. Estonian oil shale – resources and usage. *Oil Shale*, 2003, **20**(3S), 295–303. https://doi.org/10.3176/oil.2003.3S.02
3. Oja, V., Suuberg, E. M. Oil shale processing, chemistry and technology. In *Encyclopedia of Sustainability Science and Technology* (Meyers, R. A., ed.). Springer, New York, NY, 2017, 1–38. https://doi.org/10.1007/978-1-4939-2493-6_102-3
4. Hutton, A. C. Organic petrography of oil shales. In *Composition, Geochemistry and Conversion of Oil Shales* (Sanpe, C., ed.). Vol. 455. Springer Netherlands, NATO ASI Series, Dordrecht, 1995, 17–33. https://doi.org/10.1007/978-94-011-0317-6_2
5. Lille, Ü. On the origin of 5-alkyl-1,3-benzenediols in the retort oil of Estonian kukersite. *Oil Shale*, 1999, **16**(3), 231–237. https://doi.org/10.3176/oil.1999.3.04
6. Blokker, P., van Bergen, P., Pancost, R., Collinson, M. E., de Leeuw, J. W., Sinninghe Damste, J. S. The chemical structure of *Gloeocapsomorpha prisca* microfossils: implications for their origin. *Geochimica et Cosmochimica Acta*, 2001, **65**(6), 885–900. https://doi.org/10.1016/S0016-7037(00)00582-2
7. Lille, Ü., Heinmaa, I., Pehk, T. Molecular model of Estonian kukersite kerogen evaluated by ^{13}C MAS NMR spectra. *Fuel*, 2003, **82**(7), 799–804. https://doi.org/10.1016/S0016-2361(02)00358-7
8. Chu, W., Cao, X., Schmidt-Rohr, K., Birdwell, J. E., Mao, J. Investigation into the effect of heteroatom content on kerogen structure using advanced ^{13}C solid-state nuclear magnetic resonance spectroscopy. *Energy Fuels*, 2019, **33**(2), 645–653. https://doi.org/10.1021/acs.energyfuels.8b01909
9. Mets, B., Kaldas, K., Uustalu, J. M., Lopp, M. The Lille-Blokker model – an excellent tool to describe the structure of kukersite. *Oil Shale*, 2023, **40**(3), 234–243. https://doi.org/10.3176/oil.2023.3.04

10. Lopp, M., Kaldas, K. Possibilities of the direct chemical transformation of kukersite kerogen: a critical review. *ACS Omega*, 2025, **10**(36), 40740–40749. https://doi.org/10.1021/acsomega.5c04675
11. Eraghi Kazzaz, A., Hosseinpour Feizi, Z., Fatehi, P. Grafting strategies for hydroxy groups of lignin for producing materials. *Green Chemistry*, 2019, **21**, 5714–5752. https://doi.org/10.1039/c9gc02598g
12. Laurichesse, S., Avérous, L. Chemical modification of lignins: towards biobased polymers. *Progress in Polymer Science*, 2014, **39**(7), 1266–1290. https://doi.org/10.1016/j.progpolymsci.2013.11.004
13. Suota, M. J., Kochepka, D. M., Ganter Moura, M. G., Pirich, C. L., Matos, M., Magalhães, W. L. E. et al. Lignin functionalization strategies and the potential applications of its derivatives – a review. *BioResources*, 2021, **16**(3), 6471–6511. https://doi.org/10.15376/biores.16.3.Suota
14. Elnaggar, E. M., Abusaif, M. S., Abdel-Baky, Y. M., Ragab, A., Omer, A. M., Ibrahim, I. et al. Insight into divergent chemical modifications of chitosan biopolymer: review. *International Journal of Biological Macromolecules*, 2024, **277**, 134347. https://doi.org/10.1016/j.ijbiomac.2024.134347
15. Jahani, A., Jazayeri, M. H. Tailoring cellulose: from extraction and chemical modification to advanced industrial applications. *International Journal of Biological Macromolecules*, 2025, **309**, 142950. https://doi.org/10.1016/j.ijbiomac.2025.142950
16. Haq, F., Yu, H., Wang, L., Teng, L., Haroon, M., Khan, R. U. et al. Advances in chemical modifications of starches and their applications. *Carbohydrate Research*, 2019, **476**, 12–35. https://doi.org/10.1016/j.carres.2019.02.007
17. Wang, Z., Deuss, P. J. The isolation of lignin with native-like structure. *Biotechnology Advances*, 2023, 68, 108230. https://doi.org/10.1016/j.biotechadv.2023.108230
18. Guo, L., Gao, Q., Ding, J., Xiong, Z., Chen, S., Li, X. et al. Lignin: dissolution, modification, and derived materials. *International Journal Biological Macromolecules*, 2025, **309**, 142748. https://doi.org/10.1016/j.ijbiomac.2025.142748
19. Beaudoin, D., Palus, E., Konduri, M. K. R., Gagné, A. Methylation of softwood and hardwood kraft lignins with chloromethane. *RSC Advances*, 2024, **14**(4), 2293–2299. https://doi.org/10.1039/D3RA08404C
20. Sadeghifar, H., Cui, C., Argyropoulos, D. S. Toward thermoplastic lignin polymers. Part 1. Selective masking of phenolic hydroxyl groups in kraft lignins via methylation and oxypropylation chemistries. *Industrial & Engineering Chemistry Research*, 2012, **51**(51), 16713–16720. https://doi.org/10.1021/ie301848j
21. Duval, A., Avérous, L. Mild and controlled lignin methylation with trimethyl phosphate: towards a precise control of lignin functionality. *Green Chemistry*, 2020, **22**(5), 1671–1680. https://doi.org/10.1039/C9GC03890F
22. Sen, S., Patil, S., Argyropoulos, D. S. Methylation of softwood kraft lignin with dimethyl carbonate. *Green Chemistry*, 2015, **17**(2), 1077–1087. https://doi.org/10.1039/C4GC01759E

23. Xiong, S.-J., Pang, B., Zhou, S.-J., Li, M.-K., Yang, S., Wang, Y.-Y. et al. Economically competitive biodegradable PBAT/lignin composites: effect of lignin methylation and compatibilizer. *ACS Sustainable Chemistry & Engineering*, 2020, **8**(13), 5338–5346. https://doi.org/10.1021/acssuschemeng.0c00789
24. Aarna, A. J., Lippmaa, E. T. О структуре керогена прибалтийского горючего сланца (On the structure of the Baltic oil shale kerogen). *Transactions of the Tallinn Polytechnic Institute, Series A*, 1955, **63**, 3–50.
25. Tundo, P., Selva, M. The chemistry of dimethyl carbonate. *Accounts of Chemical Research*, 2002, **35**(9), 706–716. https://doi.org/10.1021/ar010076f
26. Kaldas, K., Preegel, G., Muldma, K., Lopp, M. Wet air oxidation of oil shales: kerogen dissolution and dicarboxylic acid formation. *ACS Omega*, 2020, **5**(35), 22021–22030. https://doi.org/10.1021/acsomega.0c01466
27. Derenne, S., Largeau, C., Casadevall, E., Sinninghe Damsté, J. S., Tegelaar, E. W., de Leeuw, J. W. Characterization of Estonian kukersite by spectroscopy and pyrolysis: evidence for abundant alkyl phenolic moieties in an Ordovician, marine, type II/I kerogen. *Organic Geochemistry*, 1990, **16**(4–6), 873–888. https://doi.org/10.1016/0146-6380(90)90124-I
28. Derenne, S., Largeau, C., Landais, P., Rochdi, A. Spectroscopic features of *Gloeocapsomorpha prisca* colonies and of interstitial matrix in kukersite as revealed by transmission micro-FT-i.r.: location of phenolic moieties. *Fuel*, 1994, **73**(4), 626–628. https://doi.org/10.1016/0016-2361(94)90049-3
29. Smith, B. C. The C-O bond III: ethers by a knockout. *Spectroscopy*, 2017, **32**(5). https://www.spectroscopyonline.com/view/c-o-bond-iii-ethers-knockout (accessed 2025-10-24).
30. Kogerman, P., Luts, K., Hüsse, I. *The Chemistry of Estonian Oil Shale*. Goshimtexizdat, Moscow, Leningrad, 1934.
31. Tiikma, L., Zaidentsal, A., Tensorer, M. Formation of thermobitumen from oil shale by low-temperature pyrolysis in an autoclave. *Oil Shale*, 2007, **24**(4), 535–546. https://doi.org/10.3176/oil.2007.4.05
32. Shi, J., Ma, Y., Li, S., Wu, J., Zhu, Y., Teng, J. Characteristics of Estonian oil shale kerogen and its pyrolysates with thermal bitumen as a pyrolytic intermediate. *Energy & Fuels*, 2017, **31**(5), 4808–4816. https://doi.org/10.1021/acs.energyfuels.7b00054
33. Lille, Ü., Heinmaa, I., Müürisepp, A.-M., Pehk, T. Investigation of kukersite structure using NMR and oxidative cleavage: on the nature of phenolic precursors in the kerogen of Estonian kukersite. *Oil Shale*, 2002, **19**(2), 101–116. https://doi.org/10.3176/oil.2002.2.02
34. Smith, B. C. The C=O bond, part VI: esters and the rule of three. *Spectroscopy*, 2018, **33**(7). https://www.spectroscopyonline.com/view/co-bond-part-vi-esters-and-rule-three (accessed 2025-10-24).
35. Smith, B. C. The C=O bond, part VII: aromatic esters, organic carbonates, and more of the rule of three. *Spectroscopy*, 2018, **33**(9). https://www.spectroscopyonline.com/view/co-bond-part-vii-aromatic-esters-organic-carbonates-and-more-rule-three (accessed 2025-10-24).
36. Kogermann, P. N. *On the Chemistry of the Estonian Oil Shale Kukersite*. Tartu, 1931.